Chapter 3

Study of the microscopic causes of the lag phase

3.1 Introduction

Mathematical descriptions of the lag phase already exist (see Section 1.3.3). Some of them (Baranyi and Roberts, 1994; Hills and Wright, 1994; McKellar, 1997) are based on a dynamic description of growth, by means of differential equations. Later models introduced stochastic treatments (Buchanan et al., 1997; McKellar, 2001; Baranyi, 2002), with more realistic features. Recent studies have also tried to relate individual cells' lag times with population lag time (Wu et al., 2000; Métris et al., 2003; Kutalik et al., 2005). All these models have been used to study different aspects of the lag phase, such as the influence of the medium (temperature, pH, e. a.) and the initial conditions of the inoculum.

Nevertheless, in order to develop existing models, more knowledge of the underlying biological mechanisms causing the lag must be incorporated, which requires a more complete knowledge of the behaviour of individual cells (Buchanan et al., 1997; McKellar et al., 2002). Modelling and simulation at an individual level are good tools to explore the biological mechanisms of the bacteria. This is also a good way to study the mechanistic constraints of the individual cells in depth, something not taken into account by the aforementioned mathematical and stochastic treatments (Swinnen et al., 2004).

The use of an IbM offers the possibility of identifying and studying separately different contributions to the lag phase. For instance, in this work the lag phase caused by the

state of the inoculum in terms of mean biomass and biomass distribution is isolated and studied by means of the evolution of the cellular biomass distribution during this phase; then, the lag caused by a metabolic adaptation through the enzyme synthesis is also isolated and studied. Thus, two of the five causes of the lag phase described in Section 1.1.3 are tackled.

The main concern of the present chapter is to validate INDISIM as a tool for studying the bacterial lag phase. Two microscopic causes of the lag phase are assumed and studied separately, although both of them are probably simultaneous and inseparable in real systems. Firstly, the results related to the culture biomass evolution as a microscopic cause of the lag are presented. Secondly, enzyme generation is considered as another microscopic cause, when the bacteria must carry out adaptation to a new nutrient source. Then, the qualitative variability of the lag phase with different factors is presented. The effects of the inoculum size on the culture lag phase, as well as the relationship between the individual and the collective lag phase, are introduced at the end of the chapter.

3.2 Biomass evolution and the lag phase

We start by considering inocula that have a low cellular mean mass. That is, we simulate the growth of small cells in a rich culture medium. These small bacteria are typically obtained from an overnight culture in which the stationary phase has been reached and the cells have become smaller due to the starvation conditions.

Two kinds of inocula are going to be studied: a homogeneous inoculum, in which all the cells have approximately the same mass, and a heterogeous inoculum, in which a diversity in bacterial masses exists (Fig. 2.12). In spite of the differences in the shape of the initial biomass distribution, the two inocula have almost the same initial mean mass.

The first important observed result is that, in both cases, a lag phase in the number of individuals is observed, but it is not observed in the total biomass evolution (Fig. 3.1). This is common behaviour of the cultures under some specific conditions (Cooper, 2004), and a direct consequence of our reproduction model, as it considers a threshold in mass in order to initiate the division process. In this case, as the only limitation is the initial low mean mass and no metabolic adaptation is necessary, the biomass increases from the onset, while the number of individuals begins to grow after a while. That is, the lag phase is caused by the initial low mass of the bacteria of the inocula.

INDISIM allows the observation of the evolution of the culture biomass distribution. If we plot the evolution of the homogeneous inoculum (Fig. 3.2), the different phases of the growth can be clearly distinguished. First, all the cells start increasing their mass.

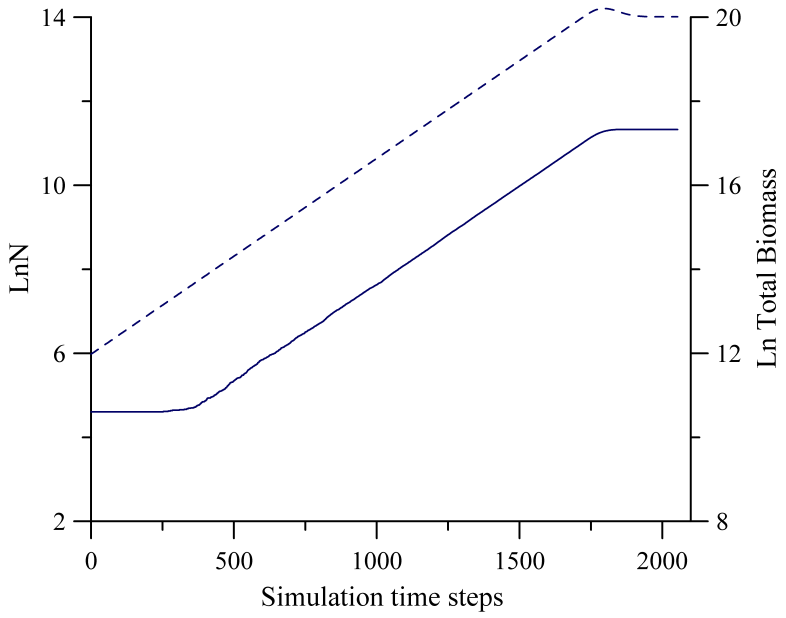

Figure 3.1: *Typical simulated curves, using INDISIM, representing the evolution of lnN (straight line) and the logarithm of total biomass (dotted line). The same slope is observed in the two curves.*

When some of the cells of the inoculum begin to divide, two different bells are observed (time step = 100 and time step = 150). The exponential phase is characterized by a stable biomass distribution: the culture is in balanced growth. At the end, when the culture enters the stationary phase, the decrease in bacterial masses is detected through a backwards shift in the biomass distribution.

3.2.1 The *distances*: a mathematical tool for assessing the evolution of the biomass distribution

As is seen in Figure 3.2, during the lag phase there is an evolution of the biomass distribution in two areas: regarding the mean mass (forwards shift of the distribution), and regarding the shape of the biomass distribution (forwards shift and widening). We need a mathematical tool to evaluate these observations and to analyze this behaviour in more detail.

On the one hand, during the lag phase the mean mass increases. Let us call $\overline{m}(t)$ the instantaneous bacterial mean mass. During the exponential growth we have observed

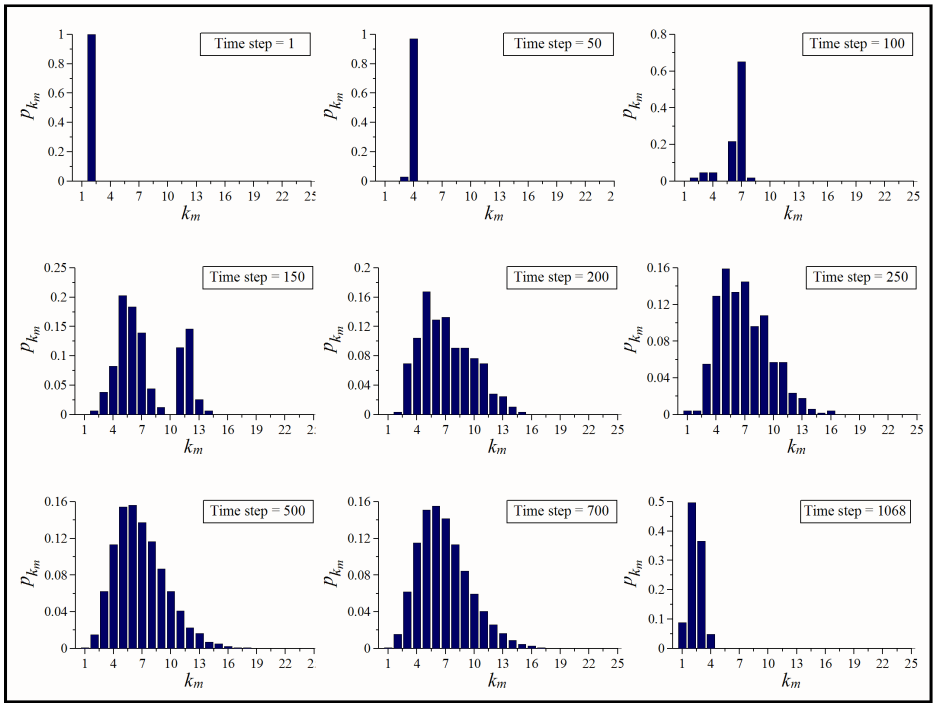

Figure 3.2: *Evolution of the culture biomass distribution from a homogeneous inoculum. In the first stages an adaptation of the distribution is observed. During the exponential phase the distribution remains constant. At the end, when the nutrient runs out, there is a backward shift of the distribution.*

that there is a constant mean bacterial biomass, $\overline{m}_{exp}$. We define the *mean mass distance* ($D_{\overline{m}}(t)$) (Eq. 3.1) in order to evaluate this change and study its relationship with the lag phase.

$$D_{\overline{m}}(t) = \frac{|\overline{m}(t) - \overline{m}_{exp}|}{\overline{m}_{exp}} \tag{3.1}$$

On the other hand, the distribution shape also changes. The instantaneous cell's biomass relative frequency is represented by $p_{k_m}(t)$. As we have observed, there is a stable distribution during the exponential phase that we call $\overline{p}_{k_m,exp}$. Thus, we define the *mass distribution distance* ($D_{p_k}(t)$) as follows (Eq. 3.2).

$$D_{p_k}(t) = \sum_{k_m=1}^{25} \left| p_{k_m}(t) - \overline{p}_{k_m,exp} \right| \tag{3.2}$$

As we presume that both evolutions are related to the lag phase, we define the *product distance* ($D(t)$) (Eq. 3.3), which takes into account the two *distances* defined above:

$$D(t) = D_{\overline{m}}(t) \cdot D_{p_k}(t) = \frac{|\overline{m}(t) - \overline{m}_{exp}|}{\overline{m}_{exp}} \cdot \sum_{k_m=1}^{25} \left| p_{k_m}(t) - \overline{p}_{k_m,exp} \right| \tag{3.3}$$

3.2.2 Analyzing the biomass distribution of a simulated growth through the *distances*

We are going to study the evolution of these *distances* in two different cultures:

1. a homogeneous inoculum with initial $\overline{m}_{t=0}/\overline{m}_R = 0.233$;
2. a heterogeneous inoculum with initial $\overline{m}_{t=0}/\overline{m}_R = 0.275$;

where $\overline{m}_{t=0}$ is the initial mean mass, and $\overline{m}_R$ is the mean mass to initiate the reproduction cycle. That is, they are two inocula with similar mean mass but different shape in biomass distribution. In each simulation, we will estimate $\overline{m}_{exp}$ and $\overline{p}_{k_m,exp}$ by calculating their mean values in the same interval of the exponential phase that is used to evaluate the equation of the line $lnN = \mu \cdot t + b$ (see Section 2.3.5). That is, we will use as typical values for these variables at exponential phase those that they have at the upper part of the growth curve, where the initial synchronism, if there was any, has been lost.

The graphic representation of the three *distances* (Fig. 3.3) shows that in both cases there is an important decrease in their values during the lag phase. Although $D_{\overline{m}}(t)$ and $D_{p_k}(t)$ seem to be good indicators in some cases, the best results are provided by the *product distance* $D(t)$. The $D(t)$ initial decrease during the lag phase is linear. In these simulations, the exponential phase of the growth begins when the $D(t)$ value is around 0.04. During the exponential growth, $D(t)$ remains near 0.

There is no constant exact value for $D(t)$ that fits in with the lag parameter, so it cannot be used as a lag measure. Nevertheless, these results show two of the phenomena that take place during the lag phase. There is an increase in the mean mass up to the typical exponential value and, at the same time, there is an adaptation of the biomass distribution to the characteristics of the exponential phase. Both are necessary in order to bring the lag phase to a close and begin exponential growth.

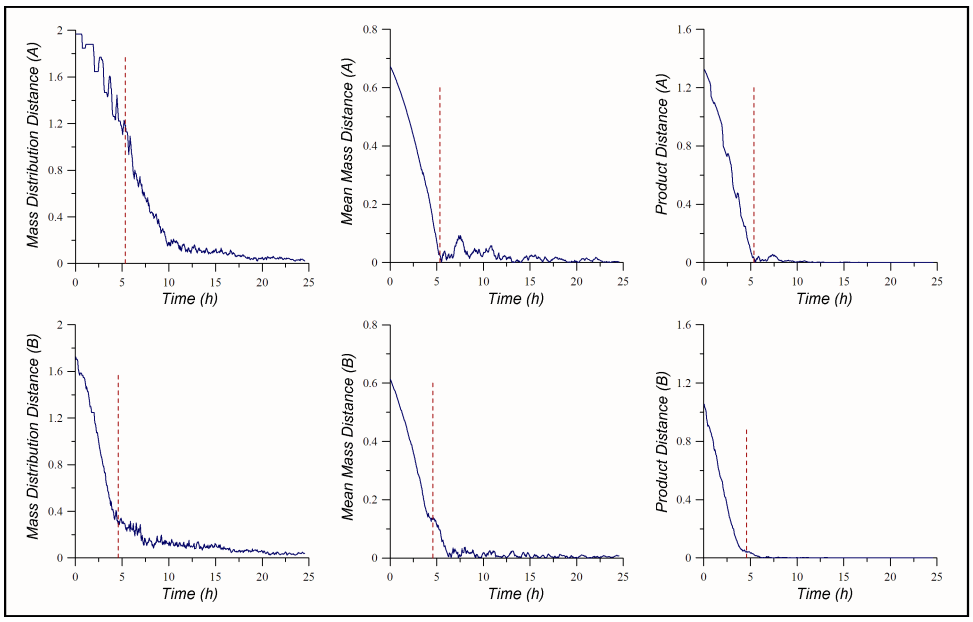

Figure 3.3: *Evolution of* mean mass distance, mass distribution distance *and* product distance *for a homogeneous (A) and a heterogeneous inoculum (B). The dotted lines indicate the lag parameter calculated in the simulation.*

3.3 Enzyme generation and the lag phase

Let us turn to a different case. Sometimes the inoculum has to adapt to a new nutrient source, because the preinoculation culture has been carried out in a different medium. In these cases, the bacteria may need to synthesize new enzymes in order to be able to take up the new substances (Pirt, 1975).

The enzyme effects are modelled as detailed in Section 2.3.3. Two kinds of generic enzyme particles are studied: intracellular enzyme particles and extracellular enzyme particles. The real systems behaviour is more complex than the proposed model, but the simplicity of the model allows a first insight toward making progress in the understanding of this kind of adaptations.

3.3.1 Evolution of the biomass distribution during the lag phase

In this section, we are going to analyze the output of simulated growth with intracellular enzyme effects. The following results are also observed in simulations with

extracellular enzymes effects.

Unlike the case studied in Section 3.2, the metabolic adaptation causes an initial decrease in the biomass which is observed in the simulations (Fig. 3.4). This is a phenomenon observed in bacteria under stress conditions (Nyström, 2004). The bacteria degrade some endogenous material to survive, with the consequent volume (and mass) reduction, while adapting themselves to the new medium.

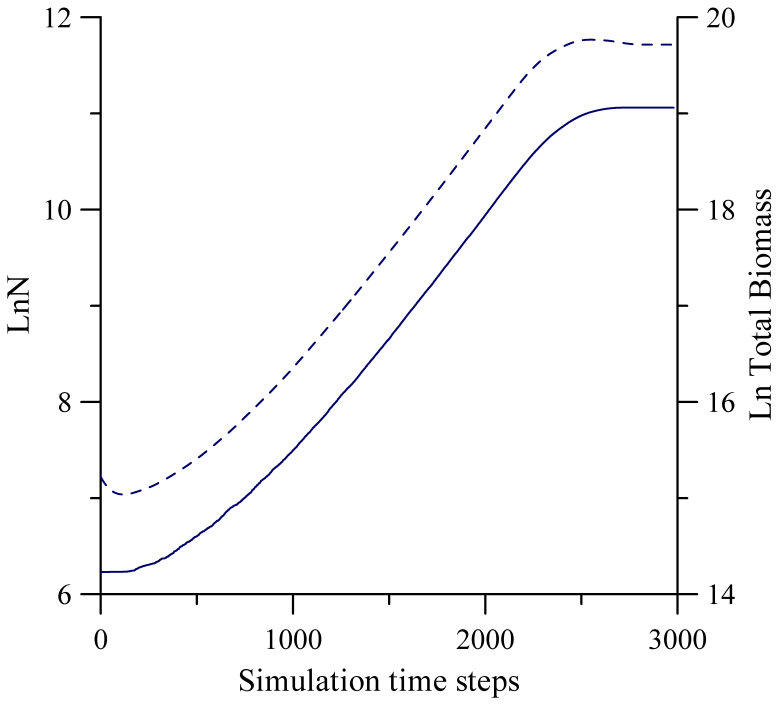

Figure 3.4: *Typical simulated curves, using INDISIM, corresponding to the adaptation with intracellular enzymes. The lag phase on lnN evolution (straight curve) and the initial decrease in the biomass (dotted curve) can be observed.*

The biomass distribution evolves according to this effect. The example of Figure 3.5 simulates the growth of an inoculum that has been taken from a culture in exponential phase and added into a different medium. Initially, it shows a backward shift. Then, once the bacteria have generated enough enzyme particles to begin taking up nutrients and increasing their biomass, the biomass distribution shows a forward shift to the characteristic exponential shape. At the end of the growth, a new backward shift reflects the starvation conditions of the bacteria.

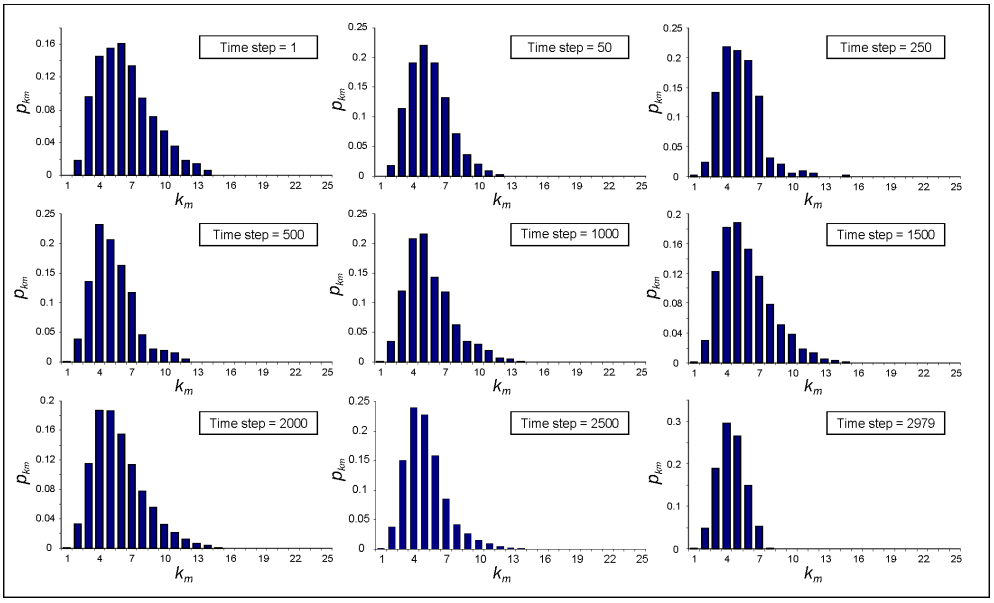

Figure 3.5: *Example of the evolution of the culture biomass distribution from a heterogeneous inoculum in a simulation for studying the effects of enzymes. An initial backward shift in the distribution is observed during the metabolic adaptation of the bacteria to the new nutrient source. Then, it resumes the same evolution as in the previous case (Fig. 3.2).*

Since the bacteria of the inoculum were growing exponentially before being added into the new medium, the changes in biomass distribution are lower than in the previous case (Fig. 3.2). This means that the three defined *distances* will be smaller. Figure 3.6 shows the evolution of the *product distance*. It starts increasing while the bacteria are performing their metabolic adaptation. Then, it can be seen that the decrease rate is slower than in the previous case. In this case the lag parameter, which is shown in the above-mentioned figure, seems to be in the middle of the adaptation period. The simulation shows a long transition between the initial lag and the exponential phase that can be observed in Figure 3.7. Actually, the curve is fully exponential by the middle of the theoretical exponential phase. These phenomena will be tackled in greater detail in later chapters.

3.3.2 Enzyme synthesis rate and lag phase

The enzyme particles may be intracellular or extracellular enzymes. Probably both of them are necessary, but we are studying them separately. Two series of simulations

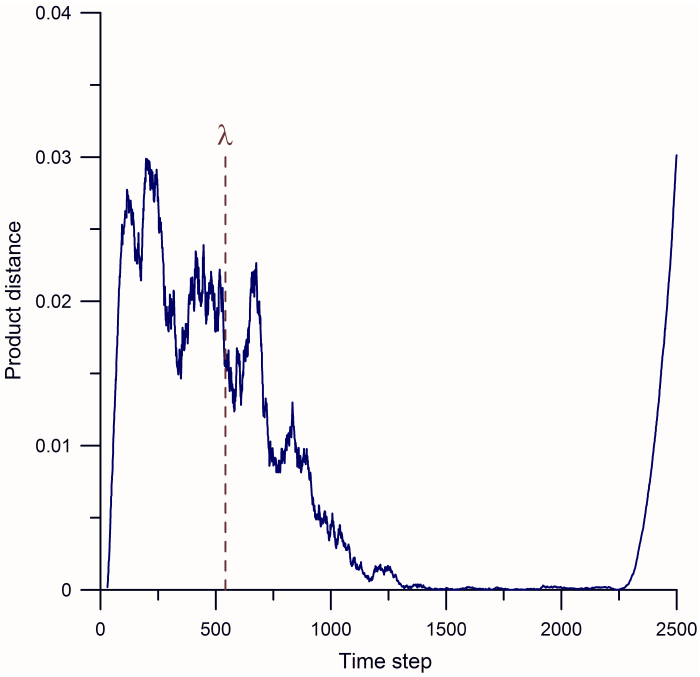

Figure 3.6: *Evolution of the* product distance *in the same simulation as Figure 3.5. An initial increase in $D(t)$ is observed, followed by a slow decrease. Then, it evolves like the previous cases (Fig. 3.3). The dotted line points out the lag parameter calculated in the simulation.*

are done, one for each type of enzyme. Specifically, our simulations relate the lag phase duration to the mean enzyme synthesis rate. The results are shown in Figure 3.8 for intracellular enzymes and in Figure 3.9 for extracellular enzymes. In these simulations, the initial biomass distribution is taken from the end phase of a previous simulation. Enzyme and nutrient particle diffusion is considered in the extracellular case, instead of the redistribution. A reference simulation with no enzyme effects has been carried out for each series, in order to isolate the low initial mass effects studied in Section 3.2. This will be a constant effect which is present in all the simulations with enzyme synthesis.

The results show that in both cases an increase in the enzyme synthesis rate produces a shorter lag phase, as expected (Fig. 3.8b and 3.9b). The main difference is found in the maximum growth rate μ_{max}. In the intracellular enzyme case, when the synthesis rate is too low the culture cannot reach the maximum growth rate permitted by the medium (Fig. 3.8c). If we consider extracellular enzymes, cooperation between bacteria is possible. This means that it is easier for the culture to reach the maximum growth rate

permitted by the medium in all simulations (Fig. 3.9c).

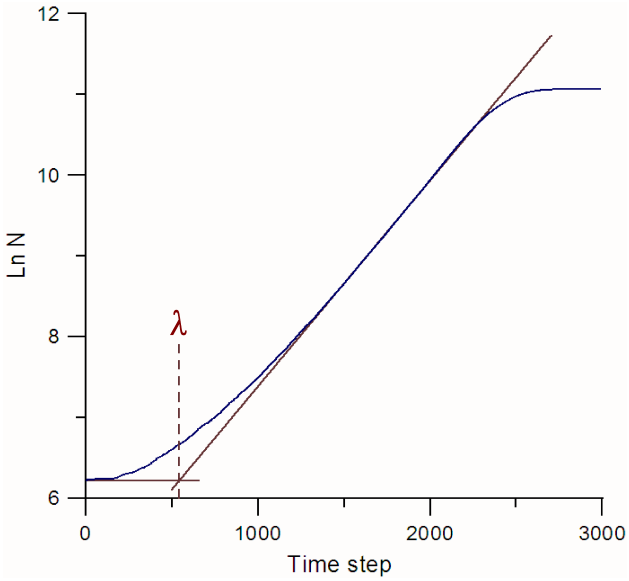

Figure 3.7: *Growth curve of the simulation example (Fig. 3.5 and 3.6). The lines that are used for obtaining the lag parameter are shown, as well as their intersection (lag parameter).*

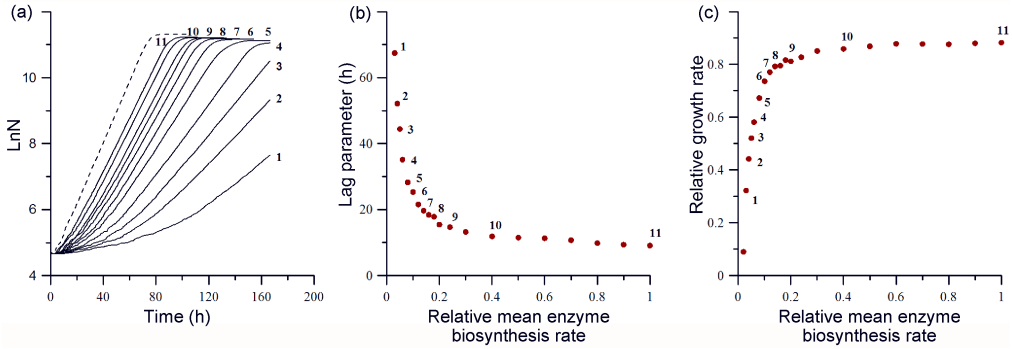

Figure 3.8: *Growth curves (lnN) of simulations performed with different intracellular enzyme generation rates (a), lag time duration versus intracellular enzyme generation rate (b), and maximum growth rate versus intracellular enzyme generation rate (c). The cardinal numbers (1-11) in the different graphs correspond to results from the same simulations. The dotted line corresponds to the reference curve, without the enzyme effect.*

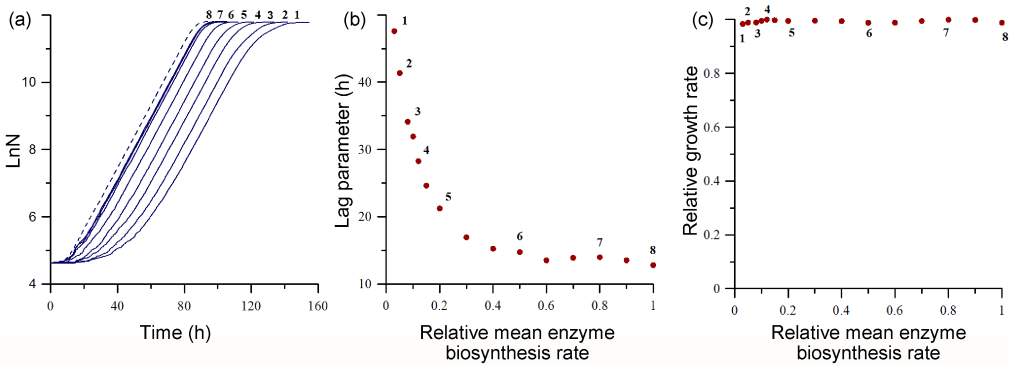

Figure 3.9: *Growth curves (lnN) of simulations performed with different extracellular enzyme generation rates (a), lag time duration versus extracellular enzyme generation rate (b), and maximum growth rate versus extracellular enzyme generation rate (c). The cardinal numbers (1-8) in the different graphs correspond to results from the same simulations. The dotted line corresponds to the reference curve, without the enzyme effect.*

3.4 Variability of the lag phase with different factors

In order to validate the suitability of our simulator, we will study the relationship of the lag phase of a homogeneous inoculum with the temperature (uptake), the initial mean mass of the inoculum, and the maintenance energy.

This is a conceptual study to validate the correct performance of the simulator and progress in the theoretical understanding of real systems.

3.4.1 Temperature

The maximum uptake constant U is related to the accessible nutrient particles around the cell (see Section 2.7). These particles are contained in a spherical volume with radius r as follows:

$$U \propto r^3 \tag{3.4}$$

This accessible volume given by r is fixed by the mean kinetic energy of the nutrient particles, which is directly related to the temperature (Allen and Tildesley, 1987), as follows:

$$r \propto \sqrt{\overline{E}_k} \tag{3.5}$$

$$\overline{E}_k \propto T \tag{3.6}$$

From Eqs. 3.5 and 3.6, a relationship between the uptake constant U and the temperature T can be deduced:

$$U \propto T^{3/2} \tag{3.7}$$

It must be stressed that Eq. 3.7 is a microbial level relationship. The results of the simulations show that the global culture behaviour is in agreement with Ratkowsky's observations (Ratkowsky et al., 1983; Ginovart et al., 2002a; Ratkowsky et al., 1982).

It has been seen that a change in the uptake constant in the simulator means a change in the simulated temperature. It can be observed that the simulator provides a good response to the changes in that parameter (Fig. 3.10): when the temperature (uptake constant) increases, the lag decreases and the maximum growth rate increases, as observed experimentally by Zwietering et al. (1994). Specifically, considering that in this work the enzyme denaturalisation temperature has not been taken into account, the simulation results fit well with the results of Ratkowsky (2003).

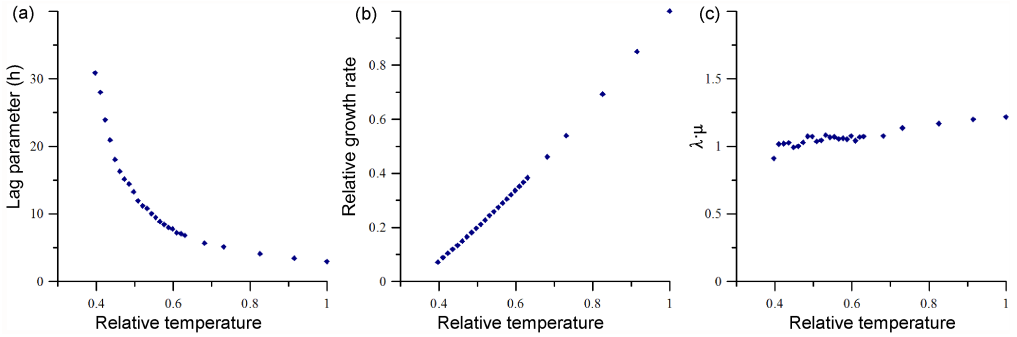

Figure 3.10: *Results of the series of simulations performed with different temperatures: lag time versus temperature (a), maximum growth rate versus temperature (b), and the product (c).*

Another important result has been obtained with INDISIM. The product $\lambda \cdot \mu_{max}$ remains approximately constant for cultures having the same initial state and growing under different (but constant) temperatures (Fig. 3.10c). This fact has been observed in several experiments and included in different models (Baranyi and Roberts, 1994). In our work the cultures follow an adaptation process from the initial mass distribution to the characteristic mass distribution of the exponential phase. In other words, the cultures must *cover* the *product distance* between the aforementioned mass distributions (Eq. 3.3). This *distance* divided by the lag phase parameter λ is the *mean velocity*

of this adaptation process. When there is no lag phase in biomass growth (there is no physiological adaptation) but there is a lag in the number of bacteria (Fig. 3.1), the characteristic parameter to evaluate the velocity of the culture's growth is the maximum growth rate μ_{max}. Therefore, $\lambda \cdot \mu_{max}$ is directly related to the *distance to be covered* by the biomass distribution.

This is an important result of INDISIM because it reproduces a macroscopic observation without having introduced any specific microscopic hypothesis. It is a proof of the consistency of the methodology used.

3.4.2 Initial cellular mean mass

The growth of inoculums with different initial cellular mean masses has been simulated. It has been noted that, while the lag phase clearly decreases when the initial mean mass increases, the maximum growth rate remains constant, which is consistent with the experimental results (Fig. 3.11). This decrease in the lag duration when the mean mass increases is due to the decrease in the distance between the initial mean mass of the inoculum and the characteristic mean mass of the exponential phase: the lower this *distance*, the shorter the time to *cover* it.

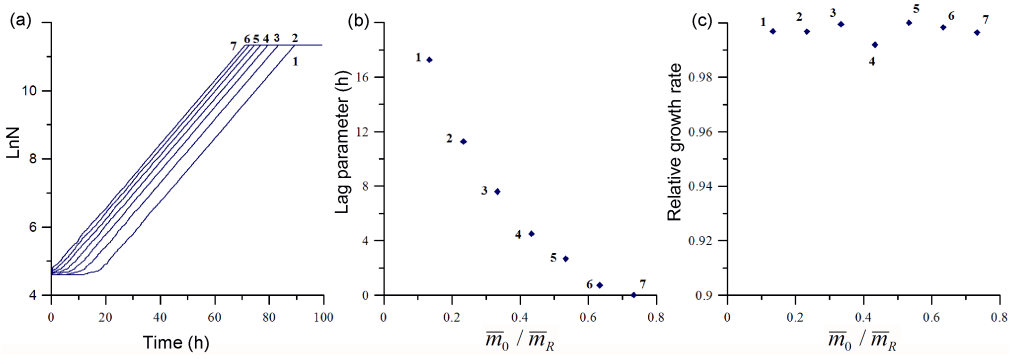

Figure 3.11: *Results of the series of simulations performed with different initial cellular mean masses ($\overline{m}_0$): growth curves (lnN) of the different simulations (a), lag time duration versus initial cellular mean mass (b), and maximum growth rate versus initial cellular mean mass (c). The mean mass to initiate reproduction cycle, $\overline{m}_R$, is taken as unit of reference.*

3.4.3 Maintenance energy

We assume that the maintenance energy is proportional to the bacteria biomass. The proportionality constant is given as a parameter. If we increase this parameter, the lag phase increases and the maximum growth rate decreases (Fig. 3.12).

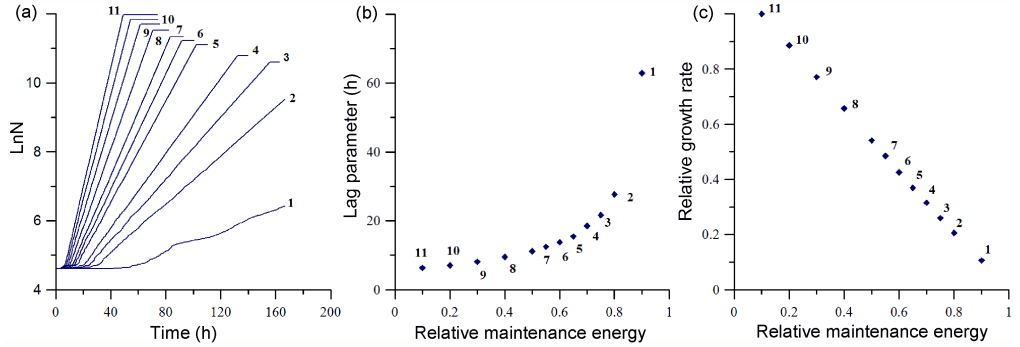

Figure 3.12: *Results of the series of simulations done with different maintenance energy constants: growth curves (lnN) of the different simulations (a), lag time duration versus maintenance energy constant (b), and maximum growth rate versus maintenance energy constant (c).*

3.5 Effects of the inoculum size

INDISIM controls each bacterium in the medium along the growth cycle. Therefore, it is especially useful for tackling the effects of inoculum size, as well as the single cell lag scope or the cell cycle duration. In this section, we use INDISIM simulations to study the inoculum size effects in the lag phase.

We have a heterogeneous inoculum of 2000 cells (Fig. 3.13). We perform different series of simulations, reproducing the potential growth of the inoculum cells after different dilutions:

- 100 simulations with an inoculum of $N_0 = 1$
- 50 simulations with an inoculum of $N_0 = 2$
- 20 simulations with an inoculum of $N_0 = 5$
- 10 simulations with an inoculum of $N_0 = 10$
- 10 simulations with an inoculum of $N_0 = 50$

- 10 simulations with an inoculum of $N_0 = 100$
- 2 simulations with an inoculum of $N_0 = 1000$

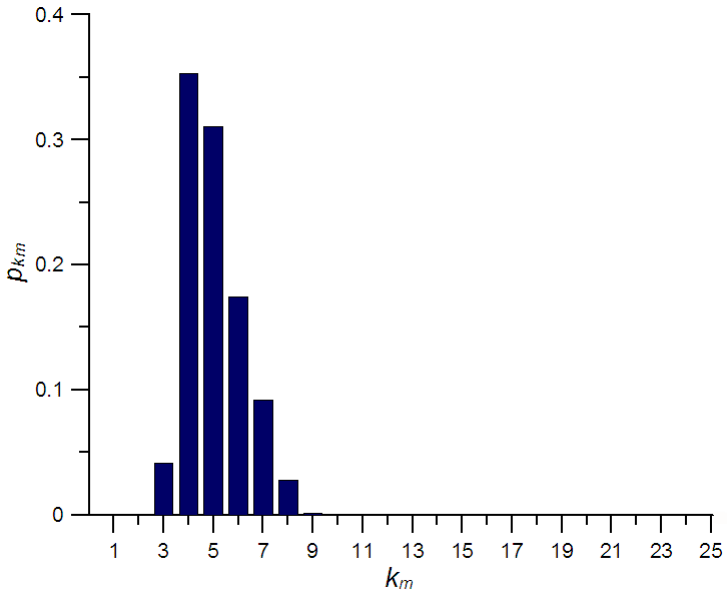

Figure 3.13: *Biomass distribution of the inoculum for the series of simulations to tackle the inoculum size effects.*

This series of simulations has been repeated for two different cases:

- without taking into account any enzyme effects. That is, the lag phase is caused by the small size of the inoculated cells.
- taking into account a metabolic adaptation to a new nutrient source. Thus, the lag phase is caused by both the small size of the inoculated cells and the enzyme synthesis effects during the first stages of the growth.

A sample of the resulting growth curves for the first case (no enzymatic adaptation effects) is shown in Figure 3.14. The growth curves for the second case (with an enzymatic adaptation) show similar behaviour with longer lags at the beginning.

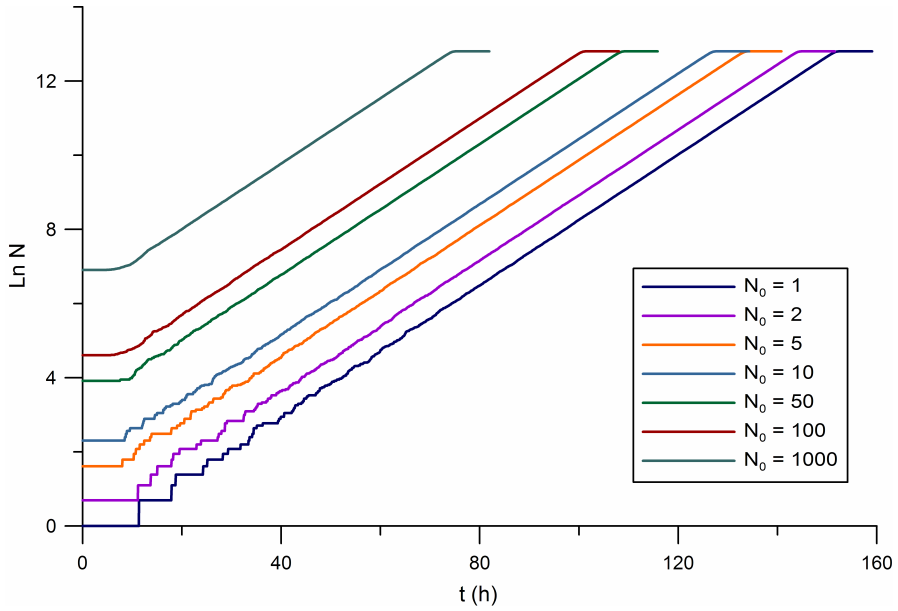

Figure 3.14: *Sample of the growth curves of the different simulated cultures with* $N_0 = 1$, 2, 5, 10, 50, 100 *and* 1000, *respectively, without considering any enzymatic adaptation. The inoculated cells are taken from the same inoculum, but grown after different dilutions.*

3.5.1 Inoculum size and the lag phase

We have evaluated the lag phase for each simulated growth curve by means of the geometrical definition, and calculated the mean lag phase parameter for each inoculum size. The simulation results do not show a decrease in the lag phase when the initial cell concentration increases. Figure 3.15 shows that the lag phase remains approximately constant and is independent of the initial cell concentration.

Several experimental results on the inoculum size effects in the lag phase have been published. Some of them show experiments in which the lag duration decreases when the inoculum size increases, which is not the case in the simulation results presented above. There are also experimental publications that show a constant behaviour of the lag duration: it is independent of the inoculum size. Robinson et al. (2001) presented a study of the inoculum size effect on the lag phase of *Listeria monocytogenes*. In this paper, when the growth took place in TSB media, the lag phase results were constant. When NaCl was added to the medium, the lag phase increased while the inoculum size decreased. Pin and Baranyi (2006) state that the variability of the lag phase with the

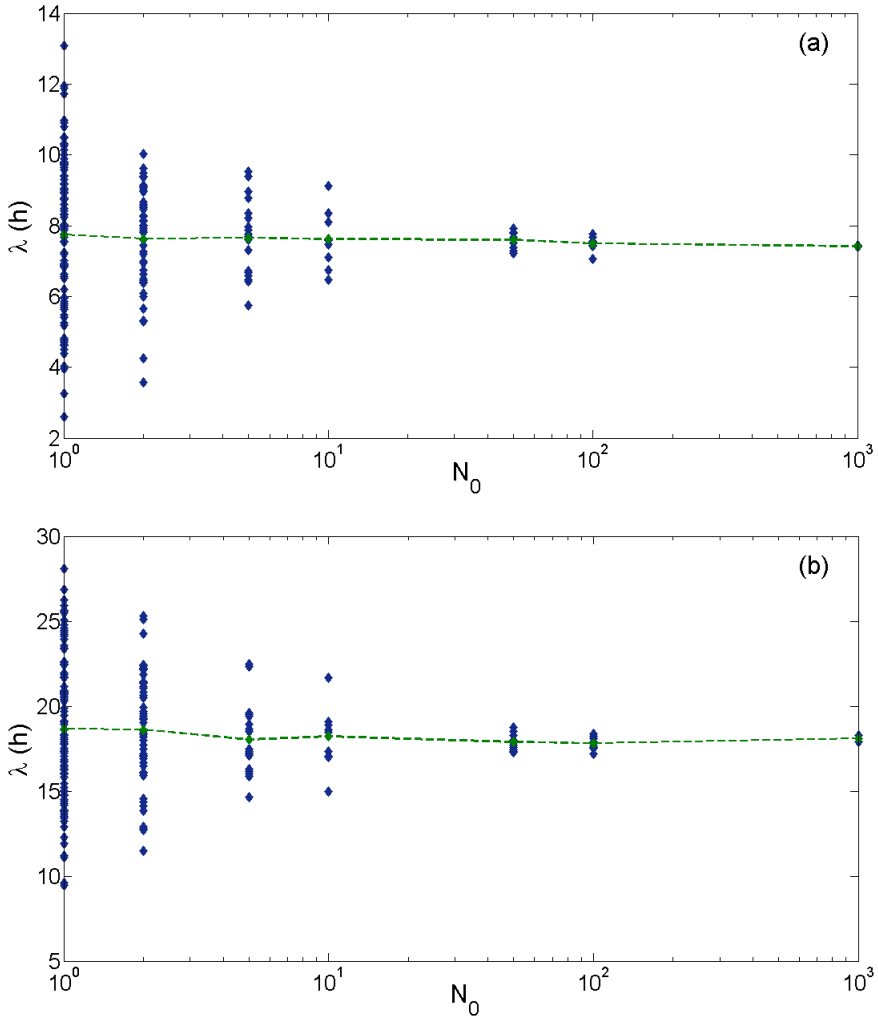

Figure 3.15: *Lag parameter, λ, versus inoculum size, N_0, without enzyme effects (a) and taking into account an enzymatic synthesis (b). The dashed line indicates the mean value for each inoculum size.*

inoculum size has been reported in several experimental studies in which the growth takes place near the growth-non growth boundary or with severely stressed inoculated cells. Actually, their experimental results do not reflect a variation of the lag phase with the inoculum size.

Inoculum size and the detection time

The detection time is an experimental parameter that is sometimes used to evaluate the lag phase of a culture when the measurements are made with optical density. It is the time when the culture reaches a fixed concentration and begins to be measurable with optical density techniques. With the simulation results we can imagine a hypothetical detection level and we can then represent this parameter versus the inoculum size. As has been experimentally shown (Robinson et al., 2001), the detection time decreases when the inoculum size increases (Fig. 3.16). In a semilogarithmic scale, a linear decrease implies no inoculum size effects on the lag phase.

Inoculum size and first division time

An interesting parameter of a growth curve is the time when the first division takes place. Therefore, we can also represent the first division time versus the inoculum size. Here, a statistical effect emerges: the mean of the first division times (t_{FD}) of the simulations with $N_0 = 1$ is much greater than the mean of the t_{FD} of the greater inocula simulations. In the high inocula we are likely to find a big cell that adapts rapidly to the new medium and, therefore, divides in the first stages of the culture growth resulting in a small t_{FD} of the culture. In contrast, the low inocula contain fewer cells: it is possible that in one repetition one of the inoculated cells is big, but the average also includes the small cells' growth. Therefore, the mean t_{FD} is much greater (Fig. 3.17) and, at the same time, the standard deviation increases.

3.5.2 Inoculum size and mean generation times

INDISIM allows the control of each bacterium in the culture. With it we know the duration of each generation for each cell - that is, the time between two consecutive divisions. Figure 3.18 shows the evolution of the individual generation times of a single simulation ($N_0 = 1000$). It may be observed that the individual first generation times are longer than those of the following generations, in accord with the existence of an initial lag phase. Then, the distribution of the individual generation times converges in a Gaussian manner during the exponential phase, when the distribution is very stable. A similar result was experimentally observed by Métris et al. (2005).

For each distribution we can calculate the mean generation time. This has been done for each generation of all the simulations of the series. Figure 3.19 shows the mean duration of the consecutive generations for the different N_0 values. The first generation has a mean duration which is considerably longer than the subsequent generations, which

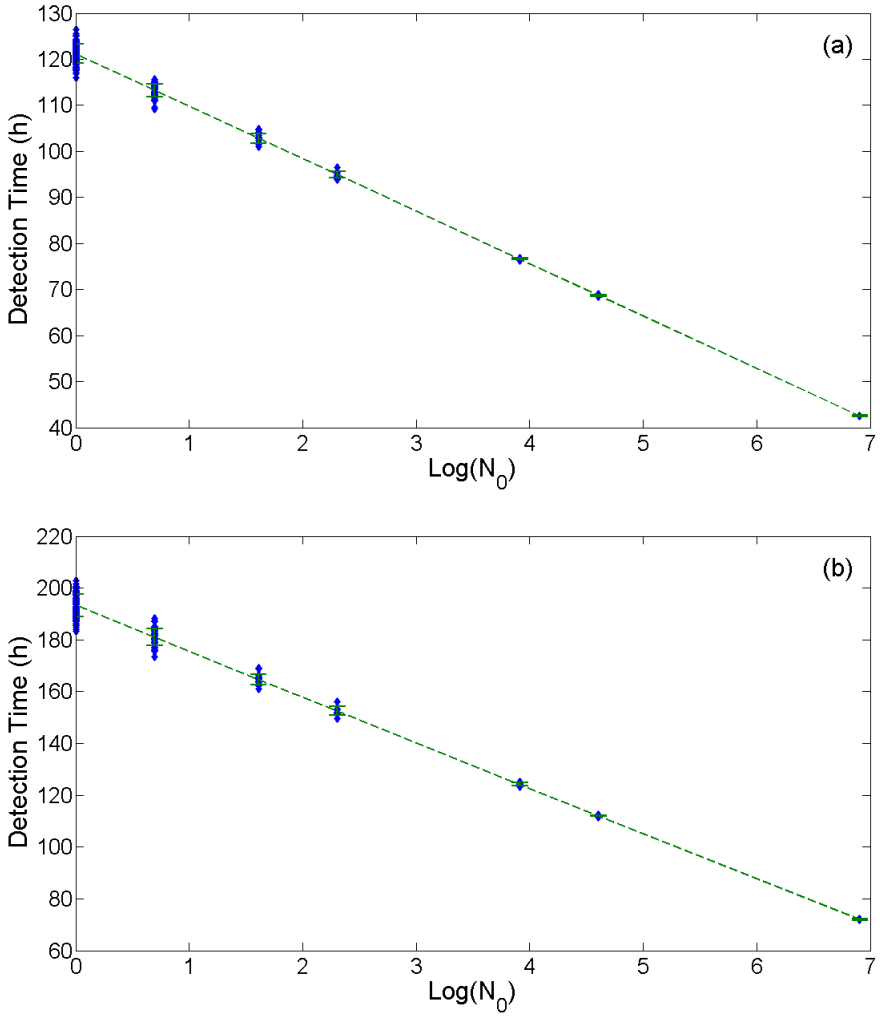

Figure 3.16: *Effect of the inoculum size on detection times without enzyme effects (a) and taking into account an enzymatic synthesis (b). The dashed line indicates the mean value for each inoculum size.*

have an approximately constant value for this parameter. This behaviour is observed in all series, independently of the N_0 value. The standard deviation also decreases with the generations. These results were experimentally observed by Métris et al. (2005).

The simulations with enzyme effects show the same behaviour, but with higher values

for the generation times (results not shown).

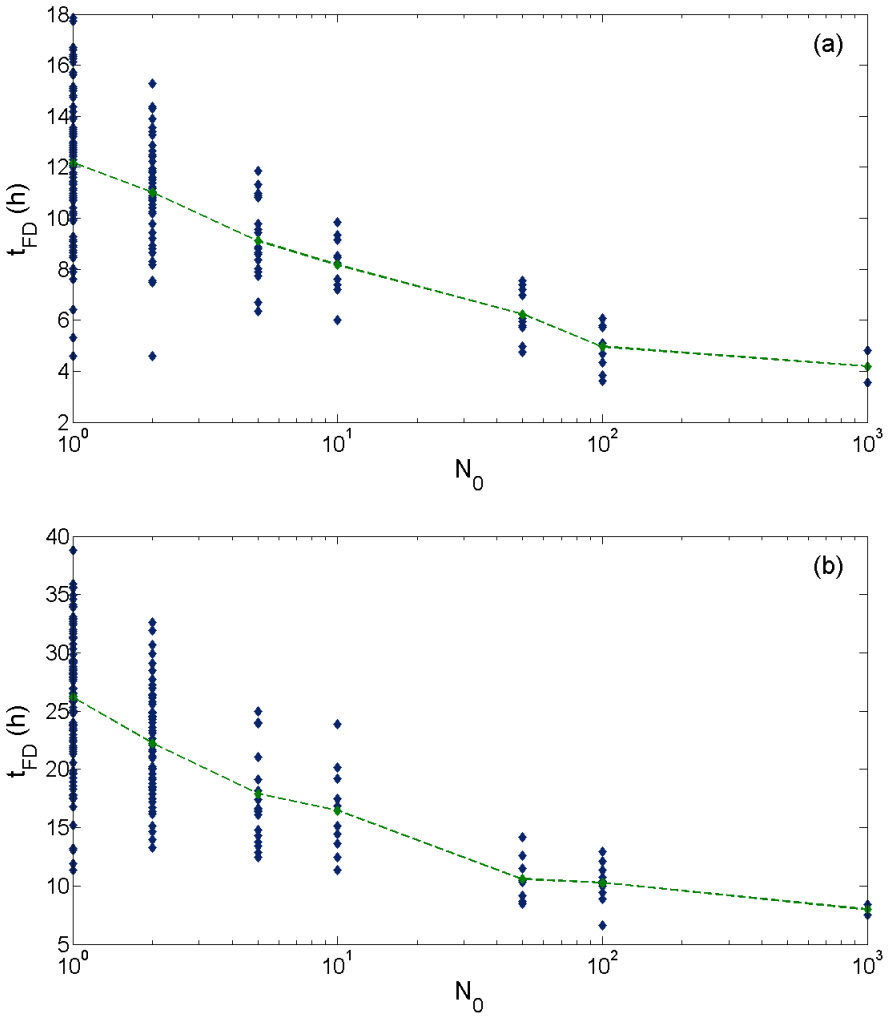

Figure 3.17: *First division time, t_{FD}, versus inoculum size, N_0, without enzyme effects (a) and taking into account an enzymatic synthesis (b). The dashed line indicates the mean value for each inoculum size.*

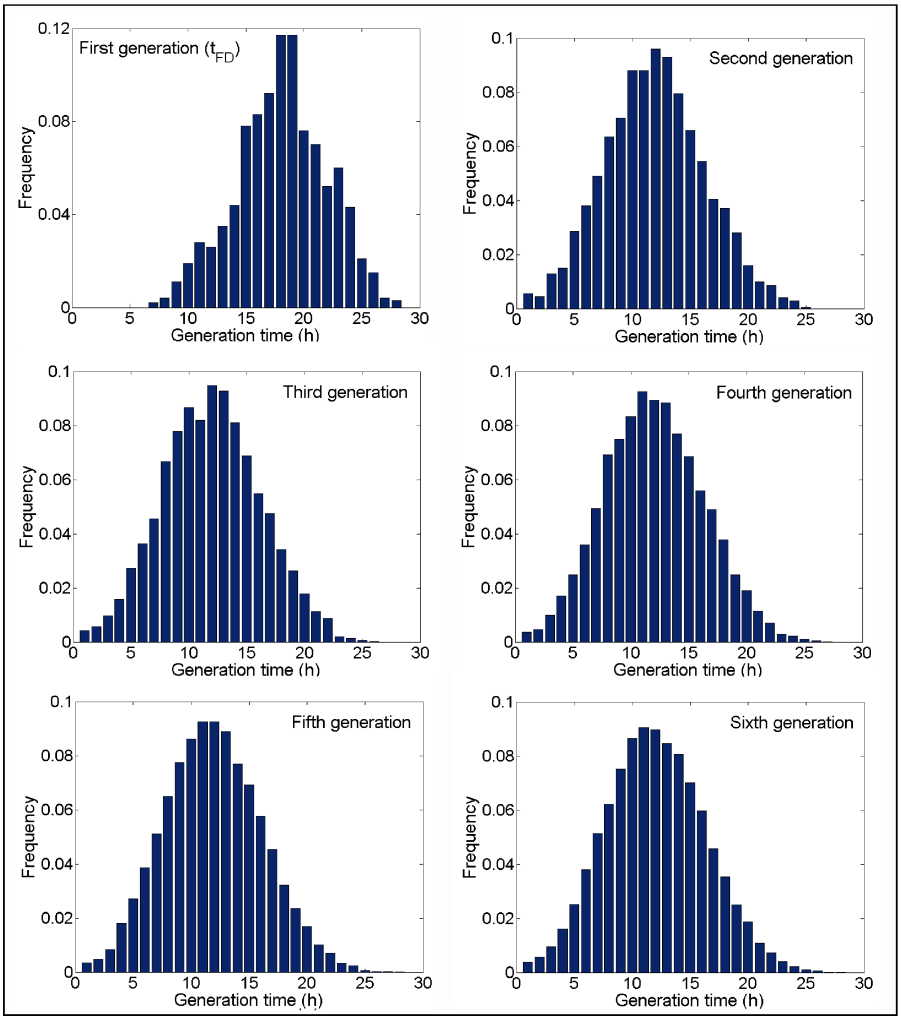

Figure 3.18: *Distribution of individual generation times for the first 6 generations of a simulation with $N_0 = 1000$. The first generation corresponds to the distribution of the times to the first division of the inoculated cells.*

Single cell lag and collective lag

Let us take now the simulations with $N_0 = 1000$. Since INDISIM controls each individual at each time step, we can follow the first division of each bacterium in the inoculum. Therefore, we can easily calculate the mean of the first generation times. It has been reported several times that the culture lag phase is lower than the mean of the

single cell lags (Baranyi, 1998; Baranyi and Pin, 2001). If we identify the single cell lags with their first division time, we find that the culture lag time is shorter than the mean of the single cell lags. In the case of the simulations with no enzyme effects, the culture lag phase is around $8\,h$ (Fig. 3.15), while the mean of the first generation duration is between $12\,h$ and $13\,h$ (Fig. 3.19). If we take the simulations where the enzyme synthesis is taken into account, the culture lag phase is around $18\,h$ (Fig. 3.15) and the mean of the first generation duration is over $25\,h$.

3.6 Discussion

Two microscopic causes of the lag phase have been described and discussed:

1. The effects of the cellular mean mass and the biomass distribution studied through two new variables: *mean mass distance* and *mass distribution distance*. With these new variables we have shown the relationship between the lag phase and the mass evolution of the culture to the exponential growth characteristics.

2. The enzymatic adaptation has also been studied, for both intracellular and extracellular enzymes. The latter has been shown to facilitate cooperation between cells.

The effect of environmental factors has shown what was already known to experimental researchers: an increase in temperature causes a decrease in the lag phase, while an increase in the maintenance constant causes an increase in the lag duration.

The reported simulation results show no dependence of the lag phase on the inoculum size. However, there is a clear decrease in detection time when the inoculum size increases, as reported by Robinson et al. (2001). The same behaviour has been observed in the first generation time versus inoculum size: in this case, it is simply a statistical effect: if the inoculum contains more cells, then it is more probable that one of them will divide early. The mean generation time over the growth period has also been studied, reproducing the experimental measures of Métris et al. (2005).

This simulator has been shown to be especially useful in the study of individual lag times. In this sense, one of the results demonstrated by Baranyi (1998) has been matched: the mean value of the individual lags is greater than the collective lag phase. Many different *thought* experiments can be carried out in this way. INDISIM is a very potent tool in the field of low-population cultures, where real experiments are still rather limited.

The suitability of this simulator in the study of the lag phase has been checked, and its potential to improve and extend the results here presented has also been examined.

Several widely known results have been qualitatively reproduced without making specific changes in the model. This is proof of the consistency of INDISIM, since the simulation outputs fit different experimental results of the literature at the same time.

Thus, INDISIM builds a bridge between individual behaviour and collective observations, and between theoretical modelling and experimental results. It is also a helpful tool in acquiring deeper understanding of cell behaviour during the lag phase.

In Chapter 5, some of the results reported in this chapter will be experimentally checked. For the moment, INIDISM has proved to be ready for further use, as will be seen in the next chapter, where it will be used to test a mathematical model for the transition from the lag phase to the exponential phase.

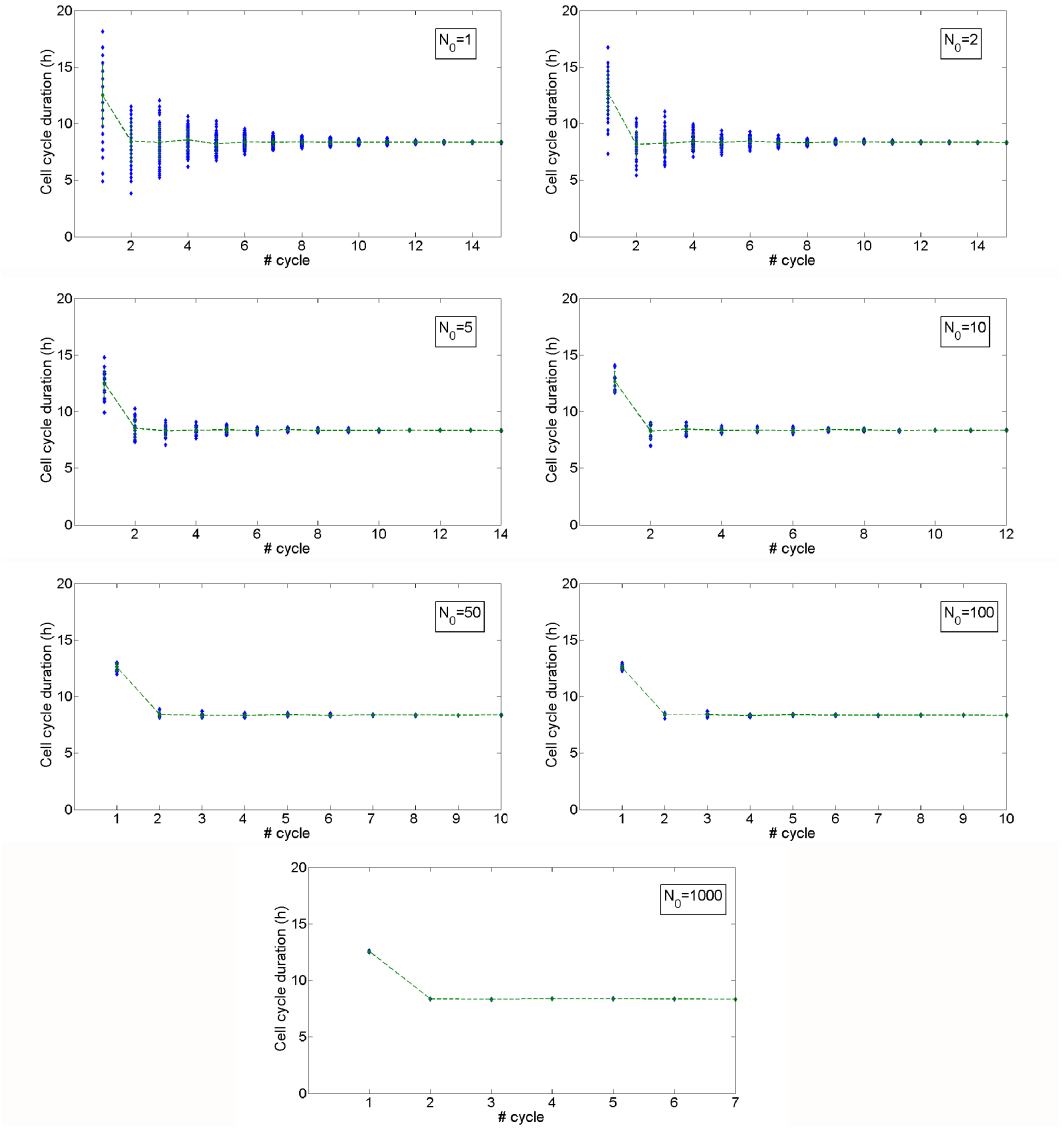

Figure 3.19: *Mean generation times for INDISIM simulations with* $N_0 = 1$, $N_0 = 2$, $N_0 = 5$, $N_0 = 10$, $N_0 = 50$, $N_0 = 100$ *and* $N_0 = 1000$. *The points correspond to the mean generation time for single simulations, and the dashed lines are the mean values for the several repetitions.*